Temperature and field dependence of the spin magnetization density in $SmMn_2Ge_2$

A. M. Bebb,[1] J. W. Taylor,[2] J. A. Duffy,[1] Z. F. Banfield,[1] M. J. Cooper,[1] M. R. Lees,[1] J. E. McCarthy,[3] and D. N. Timms[4]
[1]*Department of Physics, The University of Warwick, Coventry, CV4 7AL, United Kingdom*
[2]*ISIS Facility, The Rutherford Appleton Laboratory, Chilton Didcot, Oxon, United Kingdom*
[3]*European Synchrotron Radiation Facility, Boîte Postale 220, F-38043, Grenoble Cedex, France*
[4]*School of Earth and Environmental Science, The University of Portsmouth, Portsmouth, PO1 2DT, United Kingdom*
(Received 5 May 2004; published 12 January 2005)

The site specific spin moments in the layered intermetallic compound $SmMn_2Ge_2$ have been measured directly as a function of field, between 0.02 and 1 T, using the spin-polarized Compton scattering technique at 13, 40, and 230 K. The field dependence of the orbital moment has been determined by comparison at each temperature with magnetometry data. A small finite Sm spin moment is observed at a low applied field of 0.02 T. These data indicate that in the high-temperature ordered phase the rare-earth sites exhibit a small net moment and exhibit paramagnetic behavior with little coupling to the Mn spin sublattice. Our low-temperature, low-field data indicate a change in magnetic order of the Sm site at $\approx$35 K that is metamagnetic in nature. However, we find no evidence for a zero-field transition in the Sm sublattice as previously suggested.

DOI: 10.1103/PhysRevB.71.024407 PACS number(s): 75.25.+z

The naturally layered ternary compounds RMn_2Ge_2 have a rich *HT* phase diagram, and as such lend themselves well to investigations of interplane exchange interactions between the two separate *R* and 3*d* sublattices.[1] The interplay between the *R* and 3*d* sites, as well as the nature of the magnetic order which they exhibit, results in RMn_2Ge_2 compounds exhibiting a number of novel phenomena.[2–4] It is well known that the Sm system exhibits reenterent ferrimagnetism as well as a number of field-induced magnetic transitions related to the complex order that the Mn planes exhibit.[5] The antiferromagnetic phase of the Sm displays giant magnetoresitance[6] and as a naturally layered material, becomes a useful analog to artificially layered magnetic systems. The Sm and Gd systems have two distinct ferrimagnetic phases separated in temperature by an antiferromagnetic phase. In this paper we investigate the nature of the order of the Mn and *R* sites in the system $SmMn_2Ge_2$ in both of the ferrimagnetic phases in order to determine if the *R* sites are ordered in the high-temperature phase.

It has been proposed that the driving mechanism for the magnetism is the Mn-Mn intraplane and interplane exchange interactions.[5] In the Sm material the Mn-Mn distance is $\approx$2.87 Å, which is the critical distance for ferromagnetic ($>$2.87 Å) and antiferromagnetic order ($<$2.87 Å). Since the system is close to a magnetic instability the effect of the thermal expansion upon the unit cell volume in this material is therefore extremely important and gives rise to the rich phase diagram observed.

The magnetic phase diagram of $SmMn_2Ge_2$ shows three distinct phases. On cooling below 345 K the system orders in a ferrimagnetic structure. Previous spin-polarized Compton scattering results on this material provided evidence for a small ferromagnetically ordered Sm 4*f* spin moment in the high-temperature ferrimagnetic phase.[12] It is assumed that the Mn sublattice is a complex noncollinear arrangement of spins. At approximately 150 K the material becomes antiferromagnetically ordered, with ferromagnetic correlations between the in-plane Mn sites and antiferromagnetic order between the planes. In this phase it is assumed that the rare earth (*R*) sites are disordered. At 100 K the system orders in the reentrant ferromagnetic phase. Here the *R* site is ordered in an assumed collinear ferromagnetic arrangement, with a complex noncollinear structure on the Mn sublattice. The magnetism associated with these phases is extremely anisotropic. In the high-temperature ferrimagnetic phase the easy axis of magnetization lies along the *c* axis of the body centered tetragonal unit cell. However, in the low-temperature ferrimagnetic phase the easy axis is along the [110] direction of the crystal. The large degree of anisotropy is evidence of a strong lattice magnetism coupling that one may expect in a Sm compound.

The system studied in this investigation has prompted several questions regarding the low-temperature magnetic order. Initially questions arose over the presence of long-range order on the rare-earth site in the high-temperature ferrimagnetic phase. A previous investigation[12] in an applied field of 1 T has demonstrated that the *R* sites are ordered ferromagnetically. However, doubt remains over the possibility that the observed ferromagnetism of the *R* site is induced by the applied field used to make the measurement. Secondly it has been proposed,[7] from analysis of resistivity data, that there is a magnetic transition at $\approx$35 K in $SmMn_2Ge_2$, associated with ordering on the Sm sublattice. Again a previous measurement at 1 T has shown there to be little or no change in the magnetism at this temperature. However, the proposed transition was a minor effect that in the previous investigation was possibly washed out by the large applied field. This paper addresses both these questions.

We report a systematic study of the spin moment as a function of field at three temperatures of interest. We present field- and temperature-dependent measurements of the separated Sm and Mn magnetic sublattices at 13, 40, and 230 K, and in applied fields as low as 0.02 T. From this we deduce that there is little evidence for Sm lattice reordering at 30 K as has been reported earlier and that in the high-temperature ferromagnetic phase the Sm behaves in a paramagnetic man-

ner with a small induced moment at low field.

The Compton effect is observed when high-energy photons are inelastically scattered by electrons. The scattered photon energy distribution is Doppler broadened, since the electrons have a finite momentum distribution. If the scattering event is described within the impulse approximation,[8] the measured Compton spectrum is directly proportional to the scattering cross section.[9]

The Compton profile is defined as a 1D projection onto the scattering vector of the total electron momentum distribution $n(\mathbf{p})=n^{\uparrow}(\mathbf{p})+n^{\downarrow}(\mathbf{p})$, where the scattering vector is taken parallel to the z direction:

$$J_{\text{charge}}(p_z) = \int\int [n^{\uparrow}(\mathbf{p}) + n^{\downarrow}(\mathbf{p})]dp_x dp_y. \quad (1)$$

The integral of $J(p_z)$ is the total number of electrons per formula unit (FU). Magnetic Compton scattering (MCS) is a probe uniquely sensitive to the spin component of a material's magnetization. If the incident beam has a component of circular polarization, the scattering cross section contains a term which is spin dependent.[10] In order to isolate the spin dependence one must either flip the sample's direction of magnetization parallel and antiparallel with respect to the scattering vector or change the "handedness" of the photon helicity. Either method results in a magnetic Compton profile (MCP), $J_{\text{mag}}(p_z)$, that is dependent upon only the unpaired spin in the sample, and is defined as the 1D projection of the spin-polarized electron momentum density:

$$J_{\text{mag}}(p_z) = \int\int [n^{\uparrow}(\mathbf{p}) - n^{\downarrow}(\mathbf{p})]dp_x dp_y. \quad (2)$$

Here $n^{\uparrow}(\mathbf{p})$ and $n^{\downarrow}(\mathbf{p})$ are the momentum densities of the majority and minority spin bands. The integral of the MCP is the total spin moment per formula unit (FU) in the sample. MCS is an established technique for determining spin polarized electron densities.[11–13] Within the impulse approximation the method is insensitive to the orbital moment.[14] Unlike MXCD, MCS samples all the spin-polarized electrons regardless of their binding energies and wave function symmetries.

The magnetic Compton profiles of $SmMn_2Ge_2$ were resolved along the 001 and 110 axis of a flux grown signal crystal sample. The experiment was performed at the high-energy beamline ID15A at the ESRF. Magnetic Compton profiles were measured in reflection geometry at temperatures of 1, 40, and 230 K with the sample mounted in a closed cycle He refrigerator with Mylar windows. An incident beam energy of 220 keV was selected using a single focusing Si 311 monochromator in Laue geometry. At high photon energies ($>$150 keV), which are desirable for optimum resolution and interpretation within the impulse approximation, reversing the helicity of the incident photons is not practical. Therefore the spin-dependent signal was isolated by reversing the sample's magnetization vector using a 1 T electromagnet with the magnetic field applied along the easy axis of magnetization in each case. Circular polarization was produced by selecting a beam approximately 2 μrad below the orbital plane of the synchrotron,[15] this value being chosen to maximize the ratio of magnetic scattering to statistical noise in the charge scattering. A degree of circular polarization of about 45% was measured using a standard sample of known spin. The energy spectrum of the scattered flux was measured using a 13 element Ge detector at a mean scattering angle of $170° \pm 2°$. The momentum resolution of the magnetic Compton spectrometer, taken as the full width at half maximum (FWHM) of the instrument response function, was 0.40 a.u. (where 1 a.u. $= 1.99 \times 10^{-24}$ kg m s^{-1}), where the major component of the resolution function is the energy resolution of the Ge detector not the 1% bandwidth of the monochromating crystal.

The total number of counts in the charge Compton profiles was 2×10^8 corresponding to a statistical precision of $\pm 2\%$ in the resulting MCP, in a bin width of 0.1 a.u. Since the MCP is the difference between two charge Compton profiles, components arising from spin-paired electrons and from most sources of systematic error are effectively cancelled out. The data were corrected for energy-dependent detector efficiency, sample absorption, and the relativistic scattering cross section. The profiles were corrected for multiple scattering using the technique described by Felsteiner.[16] The magnitude of the magnetic multiple scattering was determined to be no more than 0.012%. After checking that the resulting spectra were symmetric about $p_z=0$, the profiles were folded to improve the effective statistics. The profile areas were normalized to an absolute spin moment scale using Fe data taken under the same conditions. The site specific spin moments were derived in each case by fitting a combination of a relativistic Hartree Fock (RHF) $4f$ Compton profile for the Sm ion and a RHF $3d$ Compton profile for the Mn ion, as described in Ref. 12. In this way the site moments of each of the magnetic species can be determined from the experimental data. Figure 1 shows an example of the method used to derive the Sm amd Mn contribution to the total spin moment. One should note that the RHF Compton profiles for Mn and Sm assume a spherical wave function and are calculated in the free ion approximation, hence our model does not include solid state effects. Thus there is no information about the delocalized spin moments arising from hybridization of conduction electrons by both the $4f$ and the $3d$ moments. We simply refer to the $4f$ spin and $3d$ spin inclusive of the delocalized spin moments. The fit to the data at high momenta $p_z > 5$ a.u. from free ion calculations is good, since in these regions the effects of structural symmetry on the wave function is not sampled within our resolution function. The ability to separate the conduction and the localized component to the magnetization in such systems is the topic of ongoing investigations. The values of the measured spin mo-

TABLE I. Site spin polarizations in bohr magnetons per formula unit $SmMn_2Ge_2$ at 230 K.

B[T]	Sm $4f$ M_S	$Mn3^+$ M_S and delocalized spin moment	M_L
0.02	−0.05(3)	0.26(5)	0.06(3)
0.25	−0.4(1)	3.1(1)	0.03(3)
0.5	−0.5(1)	3.1(1)	0.17(1)
1.0	−0.9(1)	3.1(1)	0.65(1)

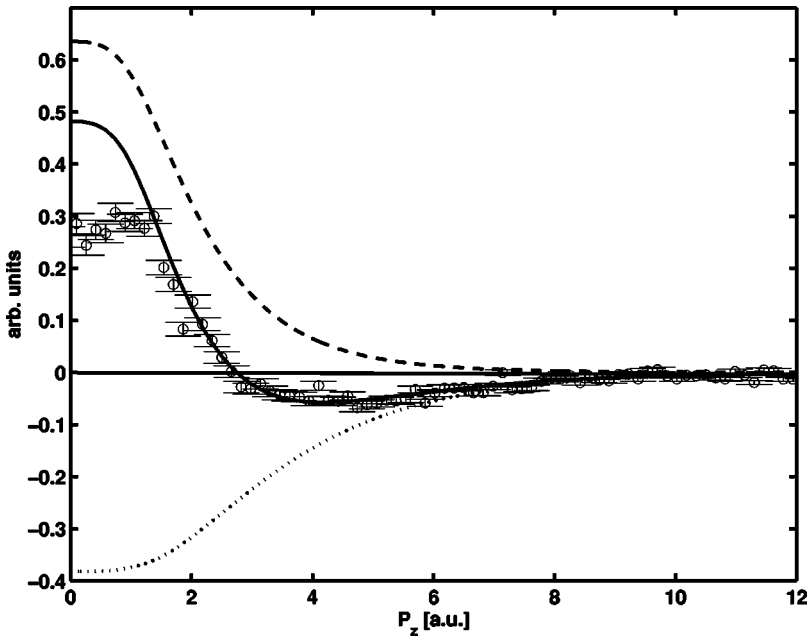

FIG. 1. Spin-resolved momentum distributions of $SmMn_2Ge_2$ ○ at 40 K resolved along the 100 direction (easy axis) with an applied field of 0.5 T. The solid line denotes the result of fitting the experimental data with a combination of Mn 3*d* dashed line and Sm 4*f* dotted line RHF Compton profiles.

ments are shown in Table I for the data set collected at 230 K. One may deduce the orbital contribution to the total moment by combining the experimentally obtained spin moments with bulk magnetization data. Since it is unlikely that the 3*d* orbital moments are totally quenched it is, with this method difficult to assertain the absoulute 4*f* or 3*d* orbital moments. The magnetization was measured on a commercially available vibrating sample magnetometer, between 0 and 1 T at 13, 40, and 230 K, with the applied field along the 110 and 001 direction (the easy axis at each respective temperature) of the crystal in order to determine the easy axis magnetization in both ferrimagnetic phases of the material. One may, by measuring the spin moment experimentally as a function of field determine the orbital and spin magnetization as a function of field. The result of this procedure is shown in Fig. 2 for data taken at 230 K. It is clear that the measured spin moment as a function of field are in good agreement with the measured total magnetization of the sample. The Sm 4*f* spin and total orbital moments are nonzero at low field, this can be taken as evidence that the Sm site may have a small net moment in zero field, and if so does not behave as a perfect paramagnet. However, it is clear the field dependence of the Sm spin moment is qualitatively different from that of the Mn 3*d* site spin (plus delocalized spin). The spin magnetization of the Sm 4*f* site increases in a linear manner with a constant susceptibility, without evidence of saturation at the maximum applied field of 1 T, unlike the total magnetic moment, which becomes saturated at $H > 0.2$ T. Interestingly the field dependence of the total orbital moment is nonlinear, indicating either a difference between the 4*f* spin and orbital susceptibility or a nonzero 3*d* orbital moment. However, our data cannot differentiate between these two

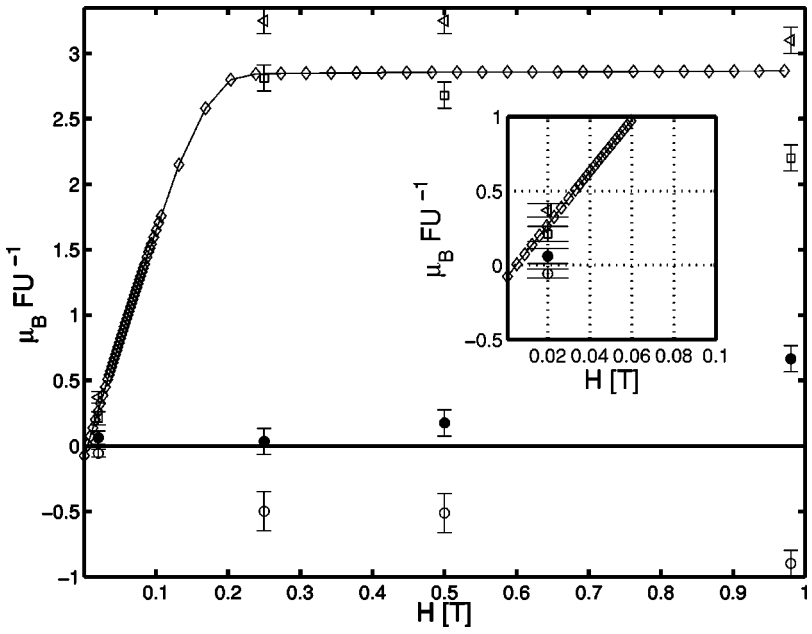

FIG. 2. Magnetic behavior of $SmMn_2Ge_2$ at 230 K. ◇, VSM magnetization; □, total spin moment; ◁, Mn contribution and delocalized spin; ○, Sm spin contribution; ●, total orbital contribution. The inset shows data in the region close to the origin.

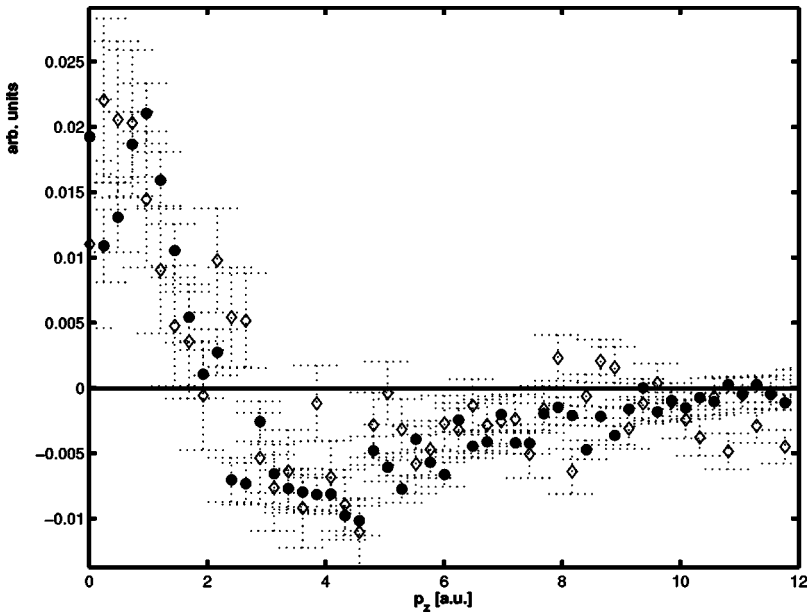

FIG. 3. Spin-resolved momentum distributions of $SmMn_2Ge_2$ at ◇=40 K and ○=13 K resolved along the 100 direction (easy axis) with an applied field of 0.05 T. The profiles are scaled to have the same Mn site contribution.

hypotheses. It is clear that $4f$ and $3d$ spin systems are well isolated with no coupling. Our data suggest that the Sm moments behave in a paramagnetic manner along the 100 direction with a strong coupling to the lattice, resulting in a high saturation field. it is assumed that at higher applied fields the Sm site moment will saturate. This can be expected from a $4f$ that is highly anisotrpic and therefore has a high degree of magnetocrystalline anisotropy.

Our data taken at low field (0.05 T at 40 and 13 K and 0.5 T at 40 and 13 K) show some evidence for a metamagnetic transition between base temperature and 40 K; however, it is clear that it is not due to the Sm sublattice ordering, as we clearly measure a Sm spin moment above and below the proposed transition temperature. The relative difference in statistical accuracy between the 0.05 and 0.5 T data, Figs. 3 and 4, respectively, results from the smaller measured moment in the low field data set. We now address the possibility of the Sm site undergoing a renormalization in the low-temperature ordered phase, as suggested earlier by resistivity data. On comparing the low-field (H=0.05 T) spin-polarized momentum distribution taken at 40 and 13 K we observe no difference in the line shape, see Fig. 3. Thus at small applied fields there appears to be no renormalization of the Sm moment since the relative contributions from Mn and Sm spins remain constant as a function of temperature. However, the data taken at 0.5 T show a line shape dependence with temperature that suggests a field induced transition associated with the Sm $4f$ moment occurring between 0.02 and 0.5 T. A small but statistically significant difference in the spin-resolved momentum distributions at 40 and 13 K, Fig. 4, in the region of 2 to 6 a.u., indicating a small difference in the magnitude of the Sm $4f$ contribution to the overall momen-

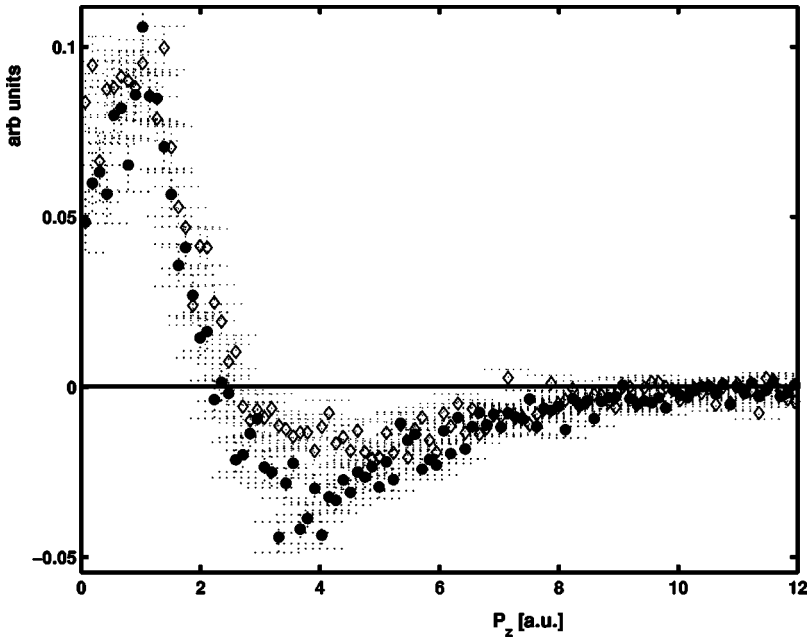

FIG. 4. Spin resolved momentum distributions of $SmMn_2Ge_2$ at ◇=40 K and ○=13 K resolved along the 100 direction (easy axis) with an applied field of 0.5 T. The profiles are scaled to have the same Mn site contribution.

tum distribution. The measured profiles, in each case (Figs. 3 and 4) have been scaled to have the same Mn site contribution. One would expect that in this case the overall line shape would be the same in each case, if the relative contributions to the spin moment remain constant. The measurements made at 0.5 T are with the system fully saturated, at both 13 and 40 K. Hence no difference should be observed due to a difference in domain populations between these two measurements. The small difference in Sm contribution to the profile can be taken to indicate a small change in the Sm site anisotropy between the two temperatures, and thus a small change in Sm site order. If the Sm site anisotropy remains constant one would expect to simply change the overall scaling factor of the two profiles, as a result of the temperature dependence of the susceptibility. However, we observe a change in only one component of the total spin moment. Thus one may assume the change in Sm site order is only a slight perturbation to the total Sm spin moment. Determination of the magnetic structure at low temperature as a function of field would elucidate the situation; however, such an experiment is difficult due to the high neutron absorption cross section of Sm.

In conclusion we have demonstrated that one may successfully extract the site specific spin and orbital moments as a function of field using the spin polarized Compton scattering technique. Furthermore, our data demonstrate that in the high-temperature phase the Sm site is ferromagnetically ordered, and not induced by the applied field used to make the measurement. In the low-temperature phase our data indicate that there is an anomaly in the low-temperature spin moments of the system between 40 and 13 K as implied by previous measurements of resistivity, however, this is not due to the Sm sublattice order as previously proposed.

The authors wish to thank the EPSRC(UK) for funding this work, the ESRF for provision of beam time, and V. Honkimaki and T. Buslaps of the high-energy beamline ID15 for their invaluable help.

[1] P. Tils, M. Loewenhaupt, K. H. J. Buschow, and R. S. Eccleston J. Alloys Compd. **279**, 123 (1998)
[2] S. B. Roy, S. Chaudhary, M. K. Chattopadhyay, P. Chaddah, and E. V. Sampathkumaran, J. Phys.: Condens. Matter **14**, 9779 (2002).
[3] Sujeet Chaudhary, M. K. Chattopadhyay, Kanwal Jeet Singh, S. B. Roy, P. Chaddah, and E. V. Sampathkumaran, Phys. Rev. B **66**, 014424 (2002).
[4] J. H. V. J. Brabers, K. H. J. Buschow, and F. R. de Boer, Phys. Rev. B **59**, 9314 (1999).
[5] J. H. V. J. Brabers, A. J. Nolten, F. Kayze, S. H. J. Lenczowski, K. H. J. Buschow, and F. R. de Boer, Phys. Rev. B **50**, 16 410 (1994).
[6] R. B. van Dover, E. M. Gyorgy, R. J. Cava, J. J. Krajewski, R. J. Felder, and W. F. Peck, Phys. Rev. B **47**, 6134 (1993).
[7] R. Mallik, E. V. Sampathkumaran, and P. L. Paulose, Physica B **230**, 731 (1997).
[8] P. M. Platzman and N. Tzoar, Phys. Rev. B **2**, 3556 (1970).
[9] P. Holm, Phys. Rev. A **37**, 3706 (1988).
[10] F. Bell and J. Felsteiner, Phys. Rev. A **53**, R1213 (1996).
[11] J. A. Duffy, S. B. Dugdale, J. E. McCarthy, M. A. Alam, M. J. Cooper, S. B. Palmer, and T. Jarlborg, Phys. Rev. B **61**, 14 331 (2000).
[12] J. E. McCarthy, J. A. Duffy, C. Detlefs, M. J. Cooper, and P. C. Canfield, Phys. Rev. B **62**, R6073 (2000).
[13] J. A. Duffy *et al.*, J. Phys.: Condens. Matter **10**, 10 391 (1998).
[14] Paolo Carra, Michele Fabrizio, Giuseppe Santoro, and B. T. Thole, Phys. Rev. B **53**, R5994 (1996).
[15] J. E. McCarthy, M. J. Cooper, P. K. Lawson, D. N. Timms, S. O. Manninen, K. Hmlinen, and P. Suortti, J. Synchrotron Radiat. **4**, 102 (1997).
[16] J. Felsteiner, P. Pattison, and M. J. Cooper, Philos. Mag. **30**, 537 (1974).